# The Effect of Creep Properties on the Oxidation Behaviour of FeAl Intermetallics at High Temperatures

C-H. Xu, W. Gao* and S. Li

*Department of Chemical & Materials Engineering,*
*The University of Auckland, New Zealand.*
** Corresponding author, e-mail w.gao@auckland.ac.nz*

(Received June 12, 2000)

## ABSTRACT

Isothermal oxidation of doped and undoped FeAl specimens was performed at 1000, 1100 and 1200°C in ambient atmosphere for 50 hours. Slip deformation occurred on the substrate of undoped FeAl at 1100 and 1200°C. Pits on the specimen surface produced by etching were used to determine the orientation of the FeAl grains. The creep strain and stress of the FeAl substrate were evaluated based on creep kinetics. The sources of creep stresses during oxidation and the orientation of the plastically deformed grains were analysed. The relationship of slip system, creep stress and grain orientation of the undoped FeAl was established. The effects of reactive elements on the properties of creep and scale spallation were also discussed.

**KEYWORDS:** A. iron aluminides (based on FeAl), B. oxidation, creep, F. electron microscopy (scanning).

## 1. INTRODUCTION

FeAl and $Fe_3Al$ are iron aluminides that possess good oxidation and sulphidation resistance /1/. They are also cheaper and lighter than stainless steels or nickel alloys. Their room temperature ductility and high temperature strength have been significantly improved by alloying /2,3/. To gain a better understanding of these promising materials, we have recently conducted a systematic study on the high temperature oxidation and sulphidation behaviours of Fe-Al, including isothermal and cyclic oxidation kinetics, scale structure and spallation tendency, and the reactive elements effects (REE) /4,5,6/.

Creep is an important mechanical property of metals at high temperatures. It also influences the oxidation properties of metals. During high temperature exposure, creep of the substrate metal can release the stresses in the oxide scale, reducing the scale spallation tendency /7/. The present paper studies the creep behaviour of FeAl during isothermal oxidation at 1000 – 1200°C, and its effects on the scale spallation property. Etched-pits and tilt SEM methods were used to determine the orientation of grains, and to study the relations of slip deformation and grain orientation /8/.

## 2. EXPERIMENTAL PROCEDURES

The chemical compositions of the test alloys are listed in Table 1. The main impurities in these alloys are Si, Mn, and Ni, which are below the level of 0.1%. Cast FeAl was annealed at 1100°C for 24 hours for homogenisation. The average grain sizes of the alloys with and without reactive elements were ~300 μm and ~800 μm, respectively. Specimens were cut from the ingots to the size of $10\times10\times1mm^3$, ground with SiC papers, polished with 3μm diamond paste.

Isothermal oxidation experiments were performed at 1000-1200°C in ambient atmosphere for 50 hours. The oxidised specimens were also electroplated with a thin Ni layer and set in epoxy resin to observe the cross

**Table 1**
Chemical compositions of the alloys (at.%)

| Specimens | Al | Zr | Y | Fe |
|---|---|---|---|---|
| Fe-37Al | 36.4 | - | - | balance |
| Fe-37Al-0.1Y | 37.7 | - | 0.10 | balance |
| Fe-37Al-0.1Y-0.2Zr | 36.8 | 0.18 | 0.06 | balance |
| Fe-37Al-0.3Zr | 36.4 | 0.25 | - | balance |
| Fe-37Al-0.8Zr | 35.3 | 0.81 | - | balance |

section micrograph. Characterisation of the oxidised specimens was performed using a scanning electron microscope (SEM).

The outside scales on the undoped FeAl specimens spalled away after isothermal oxidation for 50 hours. The oxidised specimens, after scale spallation, were etched in order to determine the crystallographic orientations of the FeAl grains. Specimen etching was conducted at room temperature for 5 min in a $Hg_2Cl$ methanol solution. After etching, the pits on the specimens were observed with SEM. The crystallographic orientations of the pit walls were determined by tilting the specimens in the SEM.

## 3. EXPERIMENTAL RESULTS

Scale spallation took place on the undoped FeAl specimens during isothermal oxidation. Slip deformation was observed on the substrate surface after oxidation at 1100 and 1200°C for 50 hours. Slip bands can be observed in some grains of FeAl substrate, Fig.1(a). A fine oxide grain layer could be seen on both the original substrate surface (marked A) and the newly exposed surface due to slip (marked B), indicating that the growth stresses in the scale caused plastic deformation. Pit-like voids formed during oxidation can be seen beneath the thin oxide layer, Fig.1(b). However, FeAl oxidised at 1000°C for 50h did not show slip deformation under SEM.

Unlike the undoped FeAl, oxide scales were still on the surface of the doped FeAl specimens after oxidation. In order to find if there is slip deformation on the doped specimens, the cross sections of the oxidised specimens

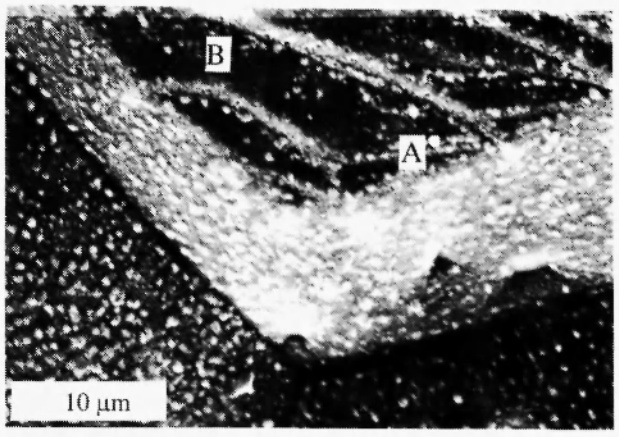


**(a)**

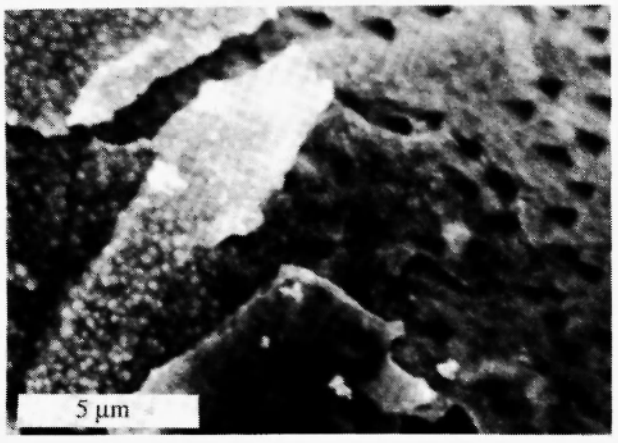


**(b)**

**Fig. 1:** SEM surface morphology of the specimens after oxidation at 1100°C for 50h, showing: (a) slip deformation in some FeAl grains of undoped FeAl and (b) the pit-like voids beneath the thin oxide layer on undoped FeAl

were observed under SEM. Fig.2(a) shows the cross section of the scales formed on the doped FeAl specimens after oxidation at 1100°C for 50 hours, exhibiting scale "pegs" formed in the scale/substrate interface. The scale/substrate interface is flat, indicating that no slip deformation took place in the substrate. Meanwhile, undoped FeAl specimens were cyclically oxidised for 50 cycles of 1h oxidation at 1100°C and 20min cooling at room temperature. The oxide scale cracked after oxidation. Slip deformation could be seen on the substrate from cross section view in Fig.2(b).

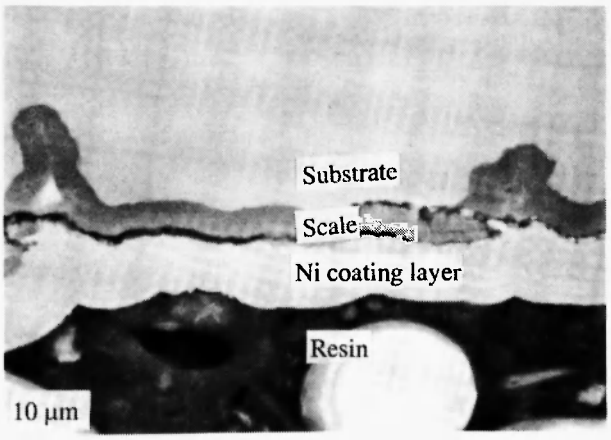


**(a)**

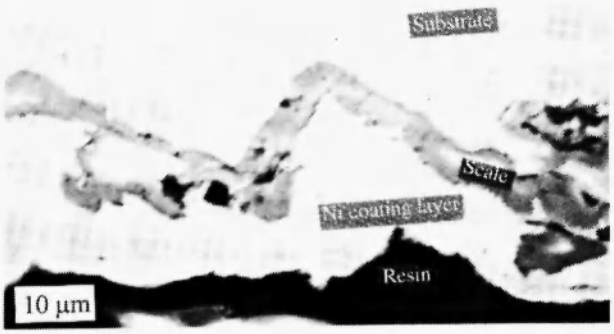


**(b)**

**Fig. 2:** Cross sections of the oxide scales on: (a) FeAl-0.3Zr after oxidation at 1100°C for 50h, showing no slip deformation and (b) undoped FeAl after 50 cycles of oxidation at 1100°C, showing the evidence of slip deformation

After the spallation of the outside scales on the undoped FeAl specimens following oxidation at 1100°C for 50 hours, the specimens were etched in the $Hg_2Cl$-methanol solution. The etched pits on the deformed FeAl grains showed a 4-fold symmetrical pyramid shape, Fig.3(a). The deformation lines can also be seen (running from the bottom-left to the top right). An FeAl grain without slip deformation was located next to a deformed grain, Fig.3(b). The etched pits show 2-fold symmetrical holes instead of the 4-fold pyramid-shape, Fig.3(a). Some of the inner oxides could still be seen on

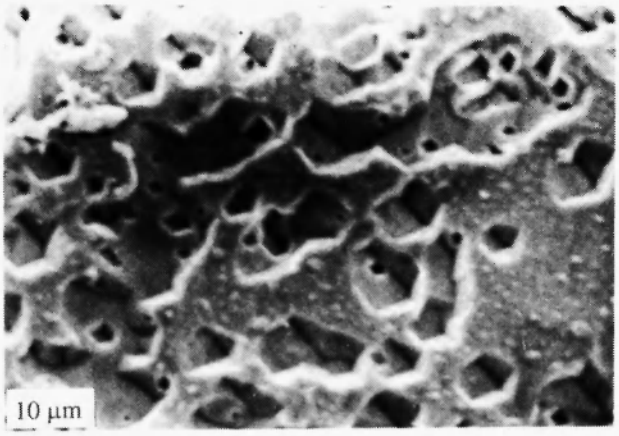


**(a)**

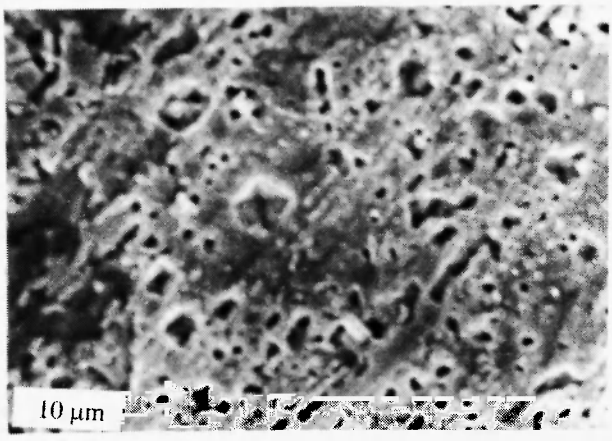


**(b)**

**Fig. 3:** Etched pits on (a) a deformed FeAl grain and (b) an undeformed FeAl grain

the specimen surface. Fig.4 shows the images of a pyramid-shape pit during tilting processes. The sample was continuously tilted from -5 to 50 degrees until the

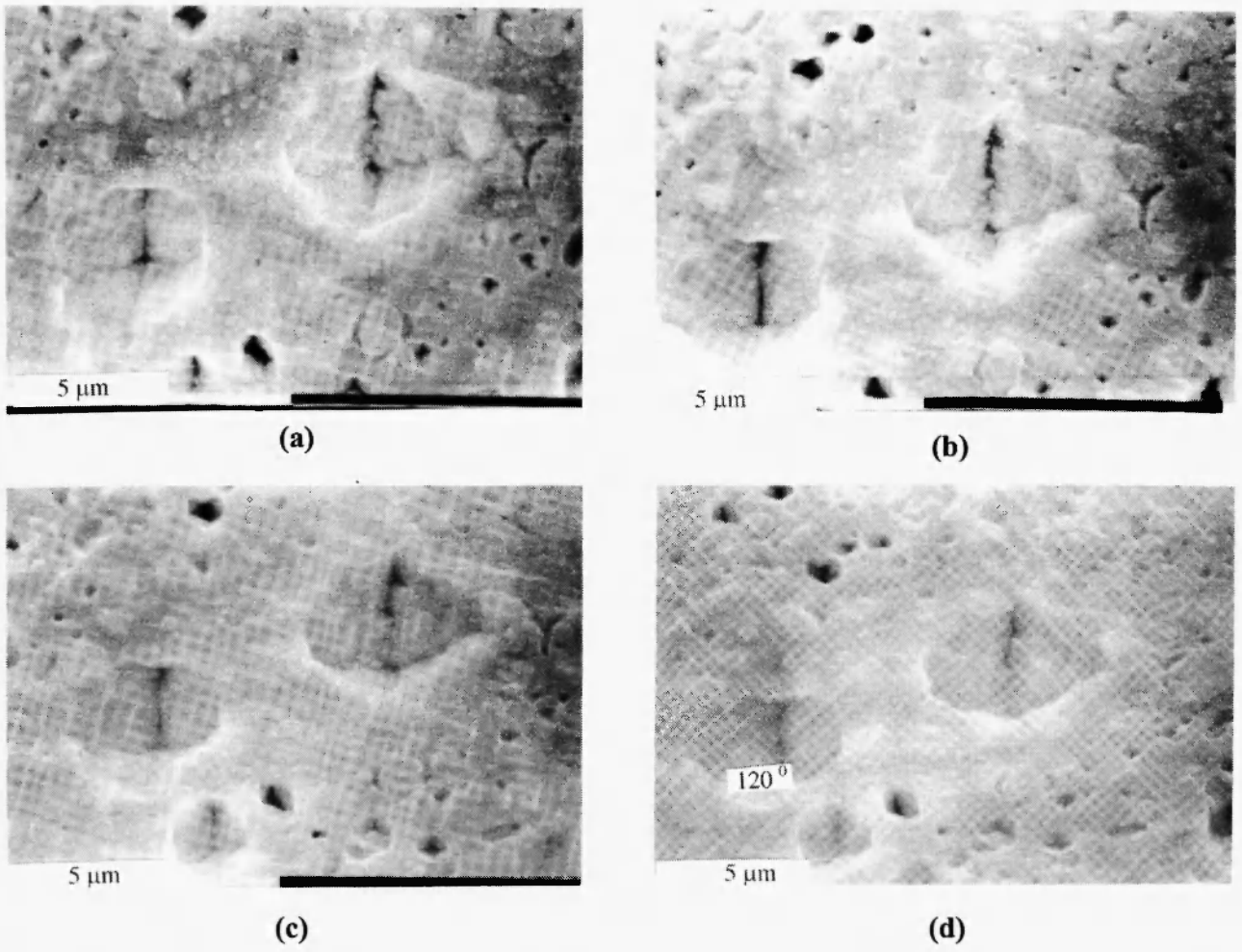


**Fig. 4:** Tilt SEM experiment for measuring the angle between two adjacent pit walls, the sample was tilted for: (a) -5°, (b) 15°, (c) 30°, and (d) 50°

adjacent two pit walls appeared to be an angled line. This measurement shows that the angle between two adjacent pit walls is 120°, Fig.4(d).

## 4 DISCUSSION

### 4.1 Creep of the Undoped FeAl

*4.1.1 Creep Kinetics*

It is believed that the activation energy of creep in FeAl is approximately equal to the activation energy of self-diffusion in pure iron. The rate controlling mechanism was found to be the dislocation climb, as was observed for pure metals /9,10/. Theoretically, ordered alloys have relatively high creep activation energies and low secondary creep rates. However, FeAl has poorer creep resistance than other intermetallics. The reason is that FeAl have a b.c.c. structure with a high concentration of constitutional defects and thermal vacancies. Therefore, pure iron creep data was used to analyse the substrate deformation of undoped FeAl.

Fig. 5 is the deformation mechanism map of pure iron /11/, showing 3 zones in the plastic deformation areas: general plastic deformation, power law creep and diffusion flow, depending on the creep stress and temperature. The deformation in the present experiment was in the high temperature area, and slip deformation was observed, Fig.1(a). Therefore the creep of the

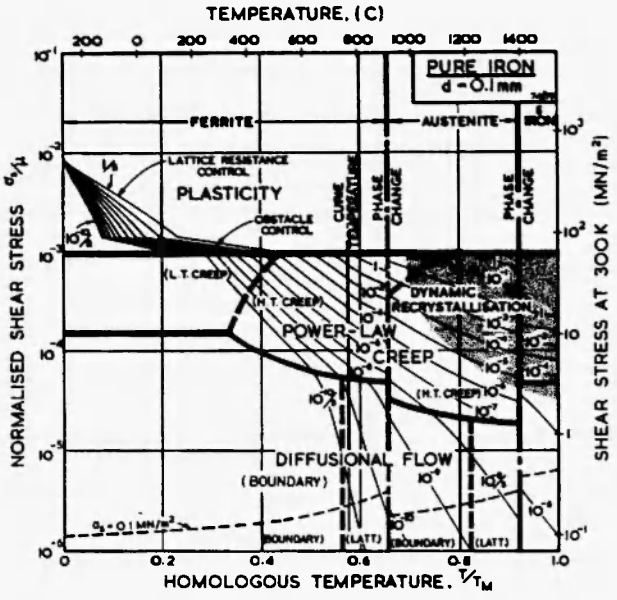


**Fig. 5:** The deformation mechanism map for pure iron with a grain size of 0.1 mm

undoped FeAl under high temperature oxidation belongs to the power law creep, consisting of dislocation slip and climb processes. It is believed that at high temperatures, dislocations can climb as well as slip to reach a higher degree of freedom. If a moving dislocation is held up by discrete obstacles, a small climb may release it, allowing it to slip to the next set of obstacles. The slip steps are responsible for almost all strain, although the average velocity is determined by the climb steps /11/. This mechanism is called "climb-controlled creep". This type of creep can be sub-divided into high temperature creep (H.T. creep), in which lattice diffusion is dominant; and low temperature creep (L.T. creep), in which the core diffusion is dominant. The power law creep is expressed in equation (1).

$$\dot{\varepsilon} = A \times e^{-\frac{Q}{RT}} \times \sigma^n \qquad (1)$$

where $\dot{\varepsilon}$ is the creep rate, $A$ is a constant, $n$ is the stress exponent, $Q$ is the activation energy. For α-Fe and δ-Fe /11/, $A = 7.0\times10^{13}$, exponent $n = 6.9$, the activation energy of lattice diffusion $Q = 251$ kJ/mol, and for core diffusion $Q = 174$ kJ/mol /11/.

The strain in a grain could be roughly evaluated with

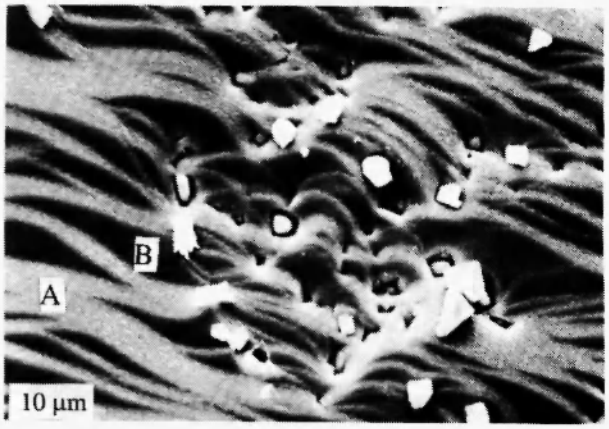


**Fig. 6:** Deformation of FeAl substrate after oxidation at 1100°C for 50h

the ratio of the newly exposed areas to the area before deformation. Creep deformation of a grain after scale spallation is shown in Fig.6 for the undoped FeAl oxidised at 1100°C for 50 hours. The initial surface areas are marked A and the newly exposed areas due to slip deformation are marked B. The ratio of B to A is estimated as ~35%, could be considered as the creep strain of a grain during oxidation. The number of grains with slip deformation is ~10% of the total grains. Therefore, the creep deformation for a specimen during oxidation is about 3.5%. The creep rate (strain/time) was therefore calculated as $0.035/(50\times3600) = 1.9\times10^{-7}$. If $T/T_m$ is more than 0.7, the creep is in the category of high temperature creep ($T_m$ = melting point). For Fe-37Al, $T_m$ = ~1500°C. At 1100°C $T/T_m$ = ~0.8, lattice diffusion activation energy (Q = 251 kJ/mole) could be used in the calculations. The creep stress on the substrate was then calculated to be 25 kN/m$^2$ using equation (1). This is much smaller than the reported residual stresses of 90,000 kN/m$^2$ in Ni oxide for Ni oxidised at 1000°C for 96 hours /12/. One of the reasons is probably that the evaluated creep stress at high temperature does not include the thermal stresses.

*4.1.2 Stresses for Creating Creep*

It is believed that the stresses for creating creep came from not only the formation of oxide scales during oxidation but also the formation of pit-like voids at the scale-metal interface. When new oxides formed inside the oxide scale on the undoped FeAl due to the diffusion

of Al and O from both sides /5/, large growth stresses were produced in the scales, resulting in buckled scales /13/. Moreover, pit-like voids in an FeAl grain with the same orientation, Fig.1(b), were observed. Due to the different atomic densities per unit area at the scale/substrate interface for FeAl grains with different orientations, stresses were generated between FeAl grains at high temperature. Furthermore, no pit-voids were observed on the substrate of undoped FeAl after oxidation at 1000°C for 50h; the specimens also did not show any slip deformation /14/. This fact implies that the stresses due to the formation of the pit-like voids may have been the main source for the slip deformation in the substrate of the undoped FeAl.

*4.1.3 Crystal Orientation of FeAl Grains*

The etched pits on the deformed FeAl grains showed a pyramid-shape, Fig.3(a). The angle between the adjacent walls of the pits was measured to be 120° (Fig.4(d)), characteristic of the {111} plane of cubic lattice, Fig.7. When the {111} plane is parallel to the paper surface, a 3-fold symmetry axis, <111>, is perpendicular to the paper surface. FeAl has a cubic lattice as shown in Fig.8. The 4-fold pyramid pit can be determined as follows. Four 3-fold symmetry axes of [1 1 1], [-1 1 1], [-1 -1 1], and [1 -1 1] are the crystallographic directions between the 4 walls of the pit based on the reference co-ordination system (X, Y, and Z). The adjacent walls of the pit are (0 -1 1) and (1 0 -1), with the angle between them is 120° /15/. Therefore, the apparently deformed grains (with the pyramid-shape pits on them) have the {100} planes parallel to the sample surface. The main slip bands were parallel to the two edges of the pits, i.e. <100> directions, as shown in Fig.3(a).

*4.1.4 Relationship of Slip System, Creep Stresses and Grain Orientation*

When temperature increases, the slip direction of FeAl changes from {011}/<111> to {011}/<100> /16/. However, recent research showed that the <100> dislocations are the result of decomposition of <111>

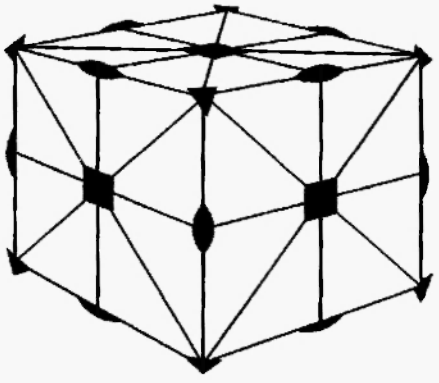

**Fig. 7:** Symmetric elements present in a cube. ▼ 3-fold symmetry directions

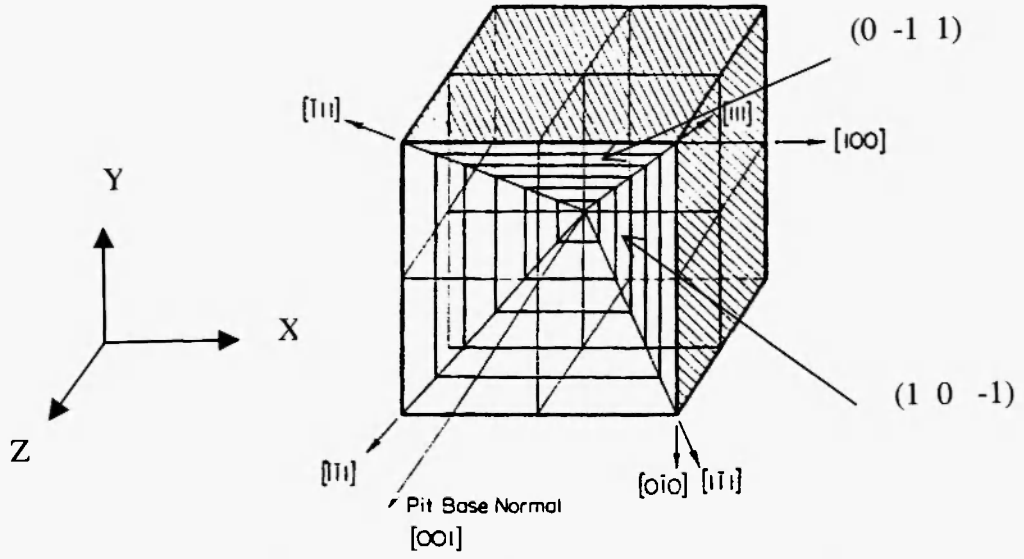


**Fig. 8:** Schematic drawing of a pit in the front face of a cube

dislocations during post-deformation cooling /17/, so {011}/<111> slip systems were used in present calculation. Plastic deformation occurs when the resolved shear stress $\tau_{RSS}$ reaches the yield strength of a single crystal.

$$\tau_{RSS} = \frac{P}{A}\cos\phi\cos\lambda \quad (2)$$

where $P$ is the applied load, $A$ is the cross section area perpendicular to the load, and $\phi$ is the angle between the load and the normal to the slip plane, and $\lambda$ is the angle between the load axis and the slip direction. For the slip system with the most favoured orientation, $\cos\phi \times \cos\lambda$ is a maximum of 0.5.

When a compressive in-plane growth stress is applied on the scale, a tensile stress with same value is generated in the substrate to balance the forces across a specimen. Assuming the scale parallel to the paper surface, for a plastically deformed grain with (0 0 1) plane parallel to the paper surface, a tensile stress $P$ was applied on the substrate, as shown in Fig.9:

$$P = p_x a_0 + p_y b_0 \quad (3)$$

where $a_0$ and $b_0$ are the unit vectors of the unit cell of lattice.

The angle between two vectors in a cube can be calculated by:

$$\cos\alpha = \frac{hu + kv + lw}{\sqrt{h^2 + k^2 + l^2}\cdot\sqrt{u^2 + v^2 + w^2}} \quad (4)$$

Therefore,

$$\cos\phi\cos\lambda = \frac{hp_x + kp_y}{\sqrt{h^2+k^2+l^2}\cdot\sqrt{p_x^2+p_y^2}}\cdot\frac{up_x + vp_y}{\sqrt{u^2+v^2+w^2}\cdot\sqrt{p_x^2+p_y^2}} \quad (5)$$

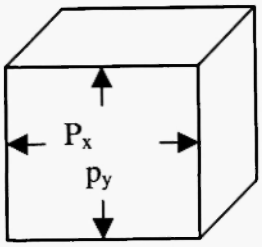


**Fig. 9:** Schematic drawing to show the stress in the metal substrate

Assuming $p_y = p_x = p$, the equation (5) becomes

$$\cos\phi\cos\lambda = \frac{h+k}{\sqrt{h^2+k^2+l^2}\cdot\sqrt{2}}\cdot\frac{u+v}{\sqrt{u^2+v^2+w^2}\cdot\sqrt{2}} \quad (6)$$

There are 12 slip systems in the {110}/<111> system. They are (1 1 0)/[1 -1 1], (1 1 0)/[-1 1 1], (1 0 1)/[-1 1 1], (1 0 1)/[1 1-1], (0 1 1)/[1 -1 1], (0 1 1 )/[1 1 −1], (-1 1 0)/[1 1 −1], (-1 1 0)/[1 1 1], (1 0 -1)/[1 -1 1], (1 0 -1)/[1 1 1], (0 1 -1)/[-1 1 1], and (0 1 -1)/[1 1 1]. Slip deformation will easily occur in the favoured slip systems with cosϕ×cosλ values close to 0.5. Using equation (3) and the slip systems {110}<111>,

$$\cos\phi\cos\lambda = 0 \quad or \quad 0.41$$

The possible values for cosϕ × cosλ in equation (6) have a maximum value of 0.41 in some slip systems, which is close to the most favoured orientation of cosϕ × cosλ = 0.5. Therefore, the slip systems with cosϕ × cosλ of 0.41 produce slip deformation. It can be derived that the growth stress on FeAl is close to the in-plane stress from the present calculation. The actual stress may be more complex than the in-plane growth stress. The scale formed on the undoped FeAl during oxidation often has bucking feature /13/. With scale bucking, both normal and shear stresses occur at the crack tips /18/.

As shown in Fig.6, large oxide grains acted as the obstacles to resist the slip process, so the dislocations could climb over the obstacles and into other slip planes. When cross slip occurred, slip offsets formed a wavy pattern.

## 4.2 Plastic Deformation on doped FeAl

As shown in Fig.2(a), no slip deformation was observed on the substrate of doped FeAl during oxidation, implying that the creep mechanism of the doped FeAl substrate is different from the undoped FeAl. When oxides grew by the anion diffusion on the doped FeAl specimens, new oxides formed at the scale/metal interface /5/, also generating growth stresses. However, it is much smaller than that when the new oxide forms in the scale. Moreover, no pit-like voids were found on the doped FeAl specimens during oxidation at high temperature, resulting in much smaller

growth stresses. Due to the small growth stresses on the scales of the doped FeAl, creep on the substrate would fall in the area of the mechanism of diffusion flow according to the deformation map (Fig.5). Therefore, creep was probably dominated by the stress-directed vacancy flow. The vacancies may flow through the grains (Nabarro-Herring creep) or along the grain boundaries (Coble creep). The present oxidation tests were conducted at temperatures over $0.4T_m$ of FeAl, so Nabarro-Herring creep should dominate the process. It has been reported that the tensile stress sharply dropped from scale/substrate interface to base metal /19/. Vacancies flew from the high tensile stress areas to the low tensile stress areas. This means that metallic atoms diffused from the base alloy to the interface. The growth stresses were able to release this way during oxidation.

On the other hand, slip deformation was not observed at the scale/substrate interface of the doped FeAl, implying that the doped FeAl alloys may have a high creep strength. It was reported that the high temperature tensile strength and creep strength in all iron aluminides were improved by dopings of Si, Ta, Ce, Ti, Mo, Zr, Hf, or Nb. Strengthening has been explained in terms of precipitation effects (pinning of grain boundaries and dislocations) because these elements have low solubility in iron aluminides and readily form intermetallic precipitates /20,21/.

### 4.3 Relation of Substrate Creep and Scale Spallation

Creep of the substrate metal influences the scale spallation tendency. Doping affects the creep properties of FeAl, therefore influencing the scale spallation resistance. Deformation of the undoped FeAl through dislocation slip and climb processes during oxidation due to the large growth stresses and low creep strength are illustrated in Fig.10(a). When a compressive stress was applied to the scale, a tensile stress was generated in the substrate to balance it. The tensile stress caused the slip deformation on the substrate. Cracks formed by pilling up the dislocations at the scale/substrate

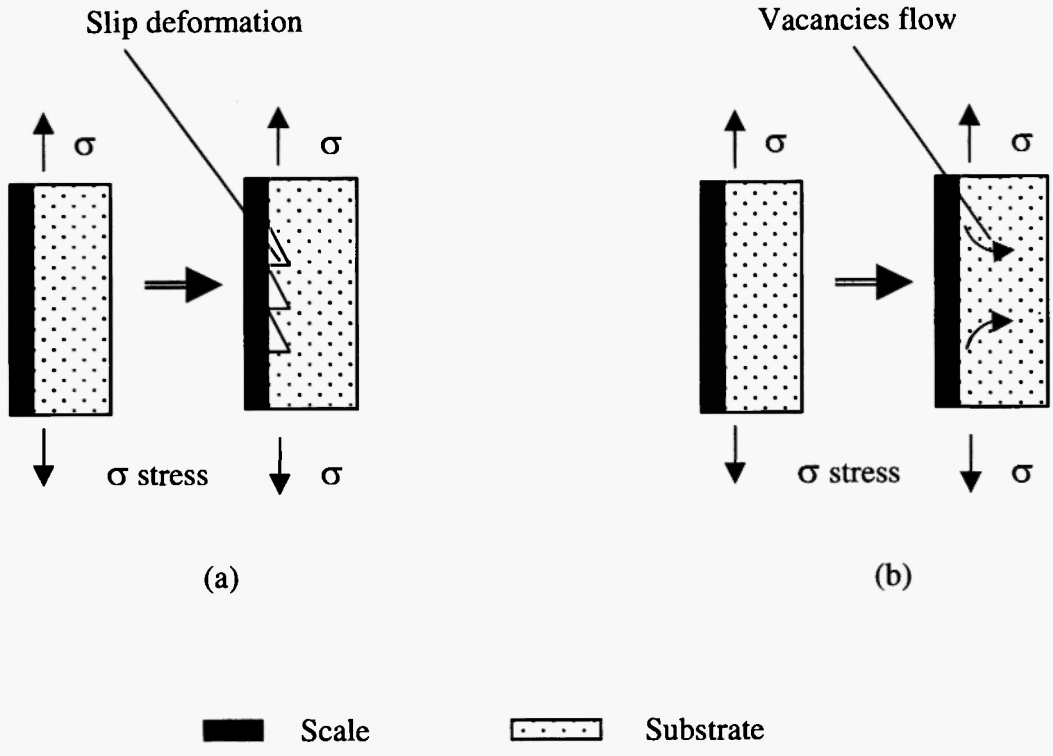


**Fig. 10:** Illustration of the creep process on the alloys during oxidation: (a) undoped FeAl, showing slip deformation speeding the scale spallation, and (b) doped FeAl, showing vacancies flow improving the scale spallation resistance

interface. Due to the weak interface strength of the undoped FeAl, the slip deformation on the substrate increases the scale failure.

For the doped FeAl, however, no slip deformation was observed on the substrate. The creep of the doped FeAl substrate belongs to the diffusion flow creep due to the low growth stress and high creep strength, as illustrated in Fig.10(b). The tensile stresses on the substrate at the interface caused vacancy diffusion from the interface to the base metal. This would release the growth stress at the scale/substrate interface, improving the spallation resistance.

## 5. CONCLUSIONS

1. Slip deformation occurs in some grains of the undoped FeAl specimens during oxidation at 1100 and 1200°C for 50 hours. Dislocations pill up at the scale/substrate interface, speeding up scale failure. For the doped FeAl, diffusion flow creep occurs on the substrate, releasing the growth stress and improving the scale spallation resistance.
2. Etched pits were used to study the crystallographic orientation of the FeAl grains. The faces of the etched pit walls were determined to be {110} planes of the FeAl cell.
3. The grains of FeAl with apparent slip deformation have a {001} lattice plane on the sample surface. The main slip bands are parallel to the <100> directions. The growth stresses were produced by the growth of oxide and formation of the pit-like voids during oxidation, causing slip deformation of the undoped FeAl.

## ACKNOWLEDGEMENTS

The authors would like to thank the Department of Chemical and Materials Engineering, and Research Centre for Surface and Materials Science for various technical support.

## REFERENCES

1. J.H. Devan, *Oxidation of High Temperature Intermetallics*, T. Grobstein and J. Doychak (Eds.), Warrendale, PA, TMS, 1989; p107.
2. V.K. Sikka et al., "Development and Commercialisation Status of Fe3Al Based Intermetallic Alloys", in: *Proc. First Int Symp. Struct. Intermet.*, 1993; p483.
3. C.G. McKamey, "Development of Iron Aluminides", in: *Proceedings of the Fourth Annual Conference on Fossil Energy Materials*, OTNL/FMP-9011, 1990; p197.
4. C.H. Xu and W. Gao, *High Temperature Materials and Process*, **18** (5-6); 351 (1999).
5. C.-H. Xu, *Thesis*, The University of Auckland, Feb., 1999.
6. Xu C-H and Gao W., *Corrosion Science and Protection Technology*, **8** (1), 26 (1996).
7. N. Birks and G.H. Meier, *Introduction to High Temperature Oxidation of Metals*, Edward Arnold, London, 1988; p122.
8. K.T. Lee, G. de Wit Morawiec and J.A. Szpunar, *Journal of Materials Science*, **30**, 1327-1332 (1995).
9. C.G. Mckamey, P.J. Masziasz and P.W. Jones, *J. Mat. Res.*, 7 (8); 2089-2106 (1992).
10. A. Lawley, J.A. Coll and R.W. Kahn, *Trans. Met. Soc. AIME*, **218**, 166-176 (1960).
11. H.J. Frost and M.F. Ashby, *Deformation Mechanism Maps, Plasticity and Creep of Metals and Ceramics*, Pergamon Press , 1982; p1-63.
12. A. Green, *Mat. Sci. and Technol.*, **8**, 159-162 (1992).
13. C.-H. Xu and W. Gao, "Oxidation behaviours of FeAl Intermetallics – The Effect of Y on the Scale Spallation Resistance", in press in *Corrosion Science* (10 / 1999).
14. C.-H. Xu and W. Gao, *High Temperature Materials and Processes* 19 (b), 371 (2000).
15. B.D. Cullity, *Elements of X-ray Diffraction*, Addison Wesley Publishing Company Inc., 1956; p72.
16. C.R. Feng and K.P. Sadananda, *Metallurgica*, **24**, 2017-2112 (1990).
17. I. Baker and P.R. Munroe, *International Materials Reviews*, **42** (5), 181 (1997).
18. A.G. Evans, G.B. Crumley and R.E. Demaray, *Oxidation of Metals*, **20** (5/6), 193-216 (1983).

19. J.J. Barnes, J.G. Goedjen and D.A. Shores, *Oxidation of Metals*, **32** (5/6), 449-469 (1989).
20. R.S. Diehm, M.P. Kemppainen and D.E. Mikkola, *Mater. Man. Proc.*, 4, 61-72 (1989).
21. U. Prakash, R.a. Buckley and H. Jones, *Scripta Metallurgica et Materialia*, **25** (10), 2249-2253 (1991).